NANO LETTERS

pubs.acs.org/NanoLett

Subeutectic Synthesis of Epitaxial Si-NWs with Diverse Catalysts Using a Novel Si Precursor

W. Molnar,[†] A. Lugstein,*[,†] P. Pongratz,[‡] N. Auner,[§] C. Bauch,[§] and E. Bertagnolli[†]

[†]Institute for Solid State Electronics, TU-Wien, Floragasse 7, A-1040 Vienna, Austria, [‡]Institute for Solid State Physics, TU-Wien, Wiedner Hauptstrasse 8/052, A-1040 Vienna, Austria, and [§]Spawnt Research GmbH, Entwicklungszentrum Wolfen, Kunstseidenstrasse 6, D - 06766 Bitterfeld-Wolfen/Goethe-University Frankfurt a.M., Max-von-Laue-Strasse 7, 60438 Frankfurt am Main, Germany

ABSTRACT The applicability of a novel silicon precursor with respect to reasonable nanowire (NW) growth rates, feasibility of epitaxial NW growth and versatility with respect to diverse catalysts was investigated. Epitaxial growth of Si-NWs was achieved using octochlorotrisilane (OCTS) as Si precursor and Au as catalyst. In contrast to the synthesis approach with $SiCl_4$ as precursor, OCTS provides Si without the addition of H_2. By optimizing the growth conditions, effective NW synthesis is shown for alternative catalysts, in particular, Cu, Ag, Ni, and Pt with the latter two being compatible to complementary metal-oxide-semiconductor technology. As for these catalysts, the growth temperatures are lower than the lowest liquid eutectic; we suggest that the catalyst particle is in the solid state during NW growth and that a solid-phase diffusion process, either in the bulk, on the surface, or both, must be responsible for NW nucleation.

KEYWORDS Nanowire, silicon, APCVD, vapor−liquid−solid, octochlorotrisilane, subeutectic

Low-dimensional nanostructures are a new class of advanced materials that have stimulated extensive research interest due to their particular physical and chemical properties and as promising building blocks for the development of novel nanodevices. Particularly semiconductor NWs appeared attractive for applications such as bio/chemical sensors,[1] light-emitting devices with extremely low power consumption,[2] nanoelectronics,[3] solar cells,[4] and catalysis.[5] However, for potential technical applications it is required to control the position and growth direction of the NWs as well as their electrical and optical properties, which strongly depend on the diameter,[6] crystallographic orientation,[7] as well as defect structure[8] of the NWs. To circumvent the problem of handling and positioning nanometer-sized objects, the interest on epitaxial grown NWs with well-controlled shape and size has therefore produced a considerable effort on synthesis techniques. Among all growth techniques, those employing vapor-phase methods like thermal evaporation,[9] laser ablation,[10] MBE,[11] or chemical vapor deposition[12] in combination with the vapor−liquid−solid (VLS)[13] method have been proven to be most versatile regarding the composition and morphology. Many different materials including elemental and compound semiconductors, oxides, carbides, and nitrides were successfully synthesized utilizing these techniques.[14]

For the VLS synthesis of Si-NWs via chemical vapor deposition (CVD), a metal droplet catalyzes the decomposition of a Si-containing precursor gas, functions as a Si reservoir by eutectic liquid formation, and finally precipitates Si-NWs due to supersaturation. Up to now, SiH_4,[12,15] $SiCl_4$,[16] and Si_2H_6[17] were used as Si precursors and in most cases gold has been the metal catalyst of choice.

To control the orientation of Si-NWs, many groups have used epitaxy from crystalline substrates.[18] For SiH_4 as Si precursor, we have shown that Au-catalyzed VLS growth of epitaxial Si-NWs impose strong demands on surface preparation and the removal of oxides before and after seed deposition appeared to be crucial for well-controlled NW growth.[19] Best results with respect to epitaxial growth of Si-NWs were achieved using $SiCl_4$ as precursor.[20] In this case the gaseous hydrochloric acid (HCl), a byproduct of $SiCl_4$ decomposition in the hydrogen atmosphere, etches the thin native oxide layer on the Si surface presenting a clean crystal surface for epitaxial NW growth. In a similar way, epitaxial Si-NWs were grown by intentionally adding HCl to the SiH_4/H_2 feed gas.[21]

In this letter, we discuss the properties of octochlorotrisilane (OCTS) for Si-NWs synthesis, which to the best of our knowledge has not been used as Si precursor yet. The Si-NWs were grown in a hot wall atmospheric pressure CVD apparatus schematically shown in Figure 1 with the indicated gas flow direction from left to right. The main components of the growth apparatus comprise a horizontal tube furnace with three separately controlled heating zones, a quartz tube connected to a gas supply, a pumping unit, and a magnetic

* To whom correspondence should be addressed. E-mail: alois.lugstein@tuwien.ac.at.
Received for review: 05/18/2010
Published on Web: 09/15/2010

DOI: 10.1021/nl101744q | *Nano Lett.* **2010,** *10,* 3957–3961

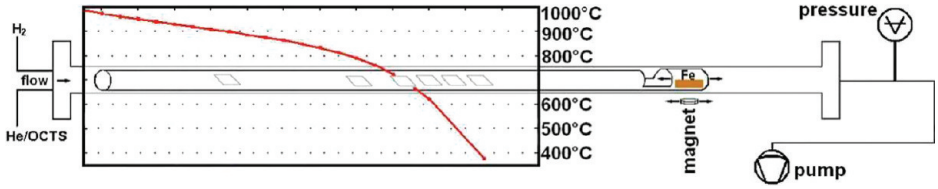

FIGURE 1. Schematic of the atmospheric pressure CVD system for the growth of Si-NWs with OCTS. The red line shows the temperature profile inside the quartz tube. The samples positioned at temperatures of 400 to 900 °C in steps of 100 °C.

specimen-transport system. This magnetic specimen-transport system enables accurate and fast in situ placement of the samples without breaking the vacuum. OCTS was added during growth via a saturator and He as feed gas.

The Si(111) substrate pieces were cleaned with acetone and isopropanol and blown dry with nitrogen. The samples were then dipped into buffered hydrofluoric acid (BHF; 7:1) to remove any native oxide followed by a water rinse. Subsequently, Au colloids with a diameter of 80 nm (Corpuscular Co.) or a 2 nm thick sputtered Au-film were deposited on the samples as VLS growth promoting catalyst. After a further BHF dip, the samples were placed on the quartz sample holder of the magnetic specimen-transport system and instantly introduced into the CVD system. After 10 min of evacuation, the tube was purged with He and the furnace was heated up. When the final growth temperature was reached, the sample holder was transferred into the growth region by the magnetic specimen-transport system. Taking into account the temperature profile and the sample position, process temperatures from 900 to 400 °C in steps of 100 °C were investigated simultaneously within the same growth sequence, which gave the most direct and reliable information about the influence of the temperature. The precursor was supplied by routing 100 sccm He through a saturator at room temperature leading to a partial pressure of 0.03 mbar OCTS in the feed gas. After typically 60 min growth, the sample holder was pulled out of the heating zone, the precursor flow was stopped and the quartz tube was purged with 200 sccm He for further 5 min.

The SEM images in Figure 2 shows the geometry and morphology of typical Si nanostructures observed at growth temperatures of 900, 800, 600, and 400 °C, when Au colloids with a diameter of 80 nm are used as catalysts.

At a growth temperature of 900 °C (Figure 2a), we observed densely grown nanorods of various appearances and sizes. For the typical growth duration of 60 min, the length and width of the rods varies typically from 2 to 20 μm and 50 to 500 nm, respectively, with a lot of kinks.

Downstream at a growth temperature of 800 °C, the NWs appeared more rodlike without kinks and more uniform in appearance with respect to length and thickness (see Figure 2b), whereby the length of the NWs was notably dependent on growth time. For the typical growth duration of 60 min, the NWs were about 8 μm long and 100−250 nm thick.

At 600 °C (Figure 2c), the substrate is covered by muscoid Si precipitations and some sparsely dispersed NWs. They are

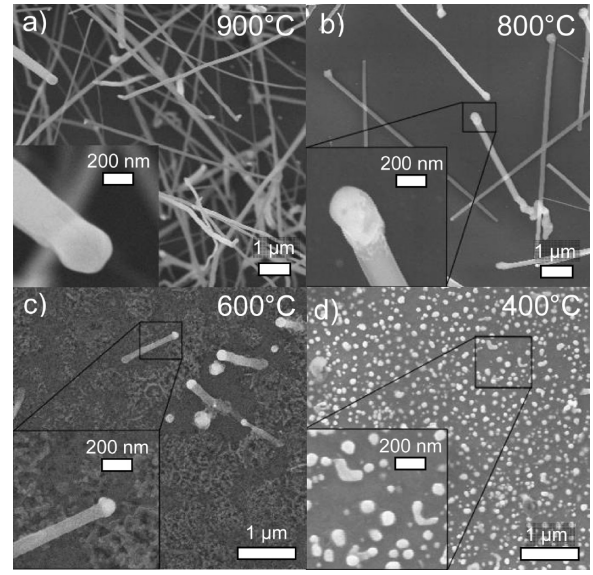

FIGURE 2. SEM images of nanostructures observed at growth temperatures of (a) 900, (b) 800, (c) 600, and (d) 400 °C (enlarged views in the inset) with OCTS as precursor using Au colloids (diameter = 80 nm) as catalyst.

much shorter with about 1 μm length and about 130 nm in diameter. Notably, for all rodlike structures grown in the temperature regime between 900 and 600 °C we observed catalytic particles atop that were identified as Au/Si alloys by means of energy dispersive X-ray (EDX).

Finally, at a growth temperature of 400 °C (Figure 2d) just the initiation of NW-growth could be observed, when tail like structures evolve from individual Au-particles.

To control the orientation of such synthesized Si-NWs, we explored epitaxy from crystalline Si-substrates.[22,23] Aside from the removal of the native oxide before and after catalyst deposition, an annealing step before growth appeared to be crucial to achieve epitaxial NW growth with OCTS as precursor. A high yield of epitaxial grown Si-NWs was achieved for a 30 min tempering of the samples at 800 °C in He atmosphere prior to the growth. The SEM images in Figure 3 show the tilted view of epitaxial Si-NWs grown for 60 min at 700 °C on Si(111) with (a) 2 nm thick sputter deposited Au layer and (b) Au colloids (80 nm) as catalyst. The NWs grow epitaxially with most of them oriented perpendicular to the substrate surface indicating a ⟨111⟩ growth direction.

The high-resolution transmission electron microscopy (HRTEM) image in Figure 3c and the selected area electron

DOI: 10.1021/nl101744q | *Nano Lett.* **2010,** *10,* 3957–3961

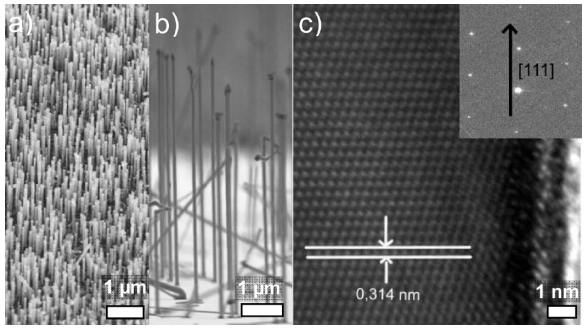

FIGURE 3. Tilted view SEM image of epitaxial Si-NWs grown at 700 °C for 60 min on Si(111) with (a) 2 nm thick sputter deposited Au layer and (b) 80 nm Au colloids as catalyst. (c) HRTEM micrograph of the single crystalline core showing clearly the Si(111) atomic planes (separation 3.14 Å) and the SAED pattern in the inset indicating the [111] growth direction.

diffraction (SAED) pattern in the inset proves that the growth axes is ⟨111⟩ for which wires vertical {112} facets have been found.[24] The HRTEM image shows further the crystalline core with the Si(111) atomic planes perpendicular to the NW axis which appeared to be free of dislocations and stacking faults.

The NWs grown with colloids as catalyst are about 10 μm long and 90 nm in diameter and appeared perfectly rodlike with no apparent uncatalytic Si deposition on the NWs or the substrate. Therefore, we suggest that uncatalyzed Si deposition does not compete with catalyzed deposition at these temperatures, thus OCTS has the potential of allowing selective Si-NW deposition. Up to now, the best results concerning epitaxially grown Si⟨111⟩ NWs on a plane substrate via the VLS growth mechanism were achieved using H_2 and $SiCl_4$ as precursor gas.[25] In this case the gaseous HCl, a byproduct of the $SiCl_4$ decomposition, etches the thin native oxide layer on the Si surface, presenting a clean Si crystal surface for epitaxial NW growth. For OCTS as a precursor due to the higher dissociation energy of the Si−Cl bond (95 kcal/mol) in comparison to the Si−Si bond (54 kcal/mol), breaking the Si−Si bond is more likely leading preferentially to $SiCl_4$ and Si.[26] In accordance with Ezhov et al.,[27] we propose a decomposition mechanism of the molecule for our synthesis process as displayed below.

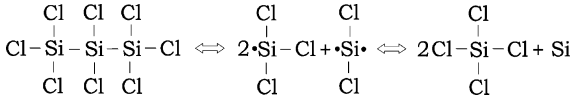

Therefore OCTS in contrast to the synthesis approach with $SiCl_4$ as precursor, provides Si without the addition of H_2.

Adding H_2 intentionally to the He/OCTS feed gas at a growth temperature of 900 °C under otherwise identical conditions leads to the formation of remarkably long and very thick Si-NWs (see Figure 4) with diameter >1 μm even though we used 80 nm colloids as catalyst (Figure 4a and

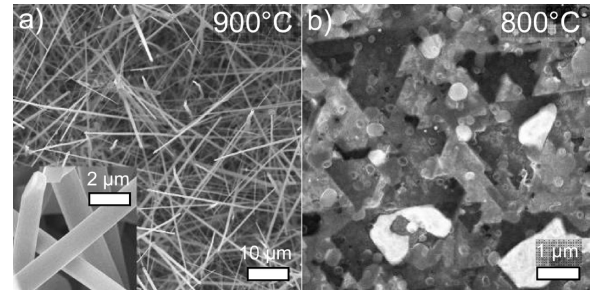

FIGURE 4. (a) Si-NWs grown with OCTS at 900 °C under H_2 atmosphere. The enlarged view in the inset shows the remarkably thick NWs with diameters >1 μm. (b) Characteristic triangular-shaped etch pits observed at 800 °C caused by the addition of H_2 to the OCTS/He feed gas.

inset). We suppose that under H_2 atmosphere the chemical byproduct $SiCl_4$ originating from the OCTS decomposition is breaking up into Si and HCl and thus makes additional Si available for growth.

Remarkably at 800 °C, the NW synthesis disappears completely if hydrogen is added and deep triangular-shaped etch pits are formed on the surface of the Si(111) substrate (see Figure 4b). This temperature appears to be too low for NW growth with $SiCl_4$ as already reported by J. Zhu et al.[28] We assume that Au further catalyzes the conversion of silicon by H_2 and OCTS into volatile products; this most likely is a mixture of SiH_2Cl_2, $SiHCl_3$, and $SiCl_4$.[29] This assumption is also supported by experiments with blank samples, i.e., no Au deposition, where under the same processing-parameters no etching was observed.

Irrespective of the Si precursor for Si-NWs synthesis via the VLS mechanism, mostly Au has been the metal catalyst of choice due to its favorable physical and chemical properties. Thereby the incorporation of Au into the NW during the synthesis cannot be eliminated and the measured upper bound on the Au concentration can be as high as 5×10^{17}−1.5×10^{18} cm^{-3}.[30] As Au is a deep level impurity in Si that significantly degrades the carrier mobility and causes fast nonradiative electron−hole pair recombination[31] the search for alternative catalysts pose a challenge. From this point of view, for OCTS as Si precursor we investigated alternative catalysts, in particular Cu, Ag, Ni, and Pt with the latter two being compatible to complementary metal-oxide-semiconductor technology.[32]

Therefore a 2 nm thick film of the respective catalyst was sputter deposited on the BHF treated Si sample. For Ag and Cu, the growth was performed under the same experimental conditions as described above at an OCTS partial pressure of 0.03 mbar. Pt as catalyst requires the addition of 20 sccm H_2 and Ni even 40 sccm of H_2 for effective Si-NW synthesis. Remarkably, for Ag and Cu the addition of traces of H_2 inhibits NW-growth. The SEM images in Figure 5 demonstrate Si-NWs growth with (a) Pt, (b) Ni, (c) Cu, and (d) Ag as catalyst.

For Pt as catalyst, effective NW growth at 900 °C requires the addition of H_2 (20 sccm) to the feed gas. For a typical

DOI: 10.1021/nl101744q | *Nano Lett.* **2010,** *10,* 3957–3961

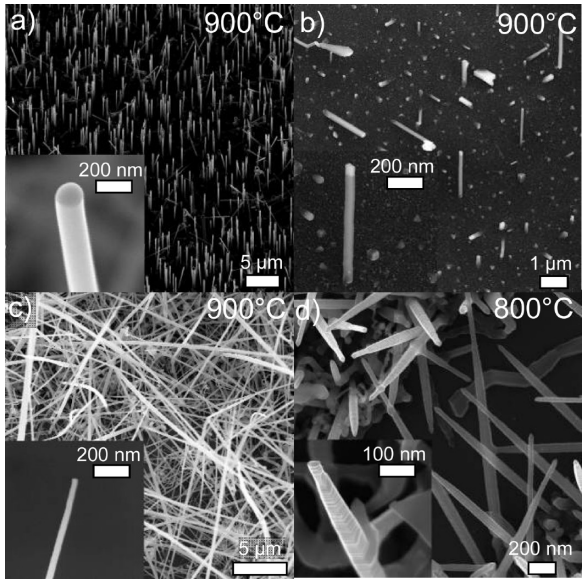

FIGURE 5. SEM images of Si-NWs grown with (a) Pt (900 °C) (b) Ni (900 °C), (c) Cu (900 °C), and (d) Ag (800 °C) and the respective insets showing a detailed view of the NW tips.

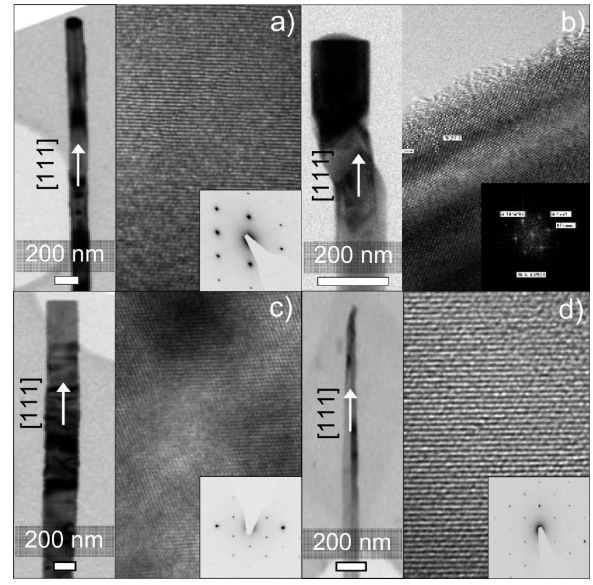

FIGURE 6. TEM images of Si-NWs grown with (a) Pt (900 °C), (b) Ni (900 °C), (c) Cu (900 °C), and (d) Ag (800 °C) as a whole are present on the respective left. The corresponding HRTEMs and FTT-pictures/ diffraction pattern to the right show their growth direction, which appeared to be [111].

growth time of 60 min, the NWs are about 6 μm long and about 160 to 200 nm thick (Figure 5a). The NWs are perfectly rodlike and the catalyst particles atop of every wire have been clearly identified by EDX as a Pt/Si alloy.

Si-NW synthesis with Ni as catalyst at 900 °C requires even more H_2 (40 sccm). The sample as a whole is just sparsely populated with NWs and the length and diameter varies over a wide range (Figure 5b). Some of the nuclei grew only a few nanometers whereas others are up to 1.5 μm long with diameters ranging from 30 to 150 nm. Most remarkable, the growth orientation of epitaxially grown NWs was identified as ⟨100⟩ and the NWs show a square-shaped cross section and blocklike bright features at the tip.

Also Cu and Ag proved to be successful growth catalysts even without adding H_2 as shown in Figure 5c,d, respectively. For Cu at 900 °C, effective Si-NW growth was achieved with wires up to 20 μm long and diameters in the range of 50 to 200 nm. The NWs are somewhat tapered and most notably we never detected any catalyst on the tips of the NWs.

Finally for Ag as catalyst, we received blocklike and preferentially close to the tip widely faceted NWs at temperatures of 800 °C. The NWs measured about 200 nm in diameter and 1 to 5 μm in length, and for all of them we identified a catalytic Ag/Si particle on top of the wire by EDX.

Figure 6 shows TEM images, detailed HRTEM images, and the respective fast Fourier transform (FFT) or diffraction pattern of the Si-NWs grown with (a) Pt (900 °C), (b) Ni (900 °C), (c) Cu (900 °C), and (d) Ag (800 °C) as catalysts.

The NWs grown with Pt as catalyst appear rodlike and are mostly free of dislocations and stacking faults. NWs grown with Ni as catalyst show a lot of twins and stacking faults, which accumulate particularly close to the catalytic particle. EDX analysis of an individual nanowire revealed pure Si and a composition of 1:2 for Si:Ni for the catalytic particle.

For both Pt and Ni catalyzed Si-NWs, the TEM shows a catalytic particle atop of the NWs. The HRTEM micrographs of the crystalline core show clearly the Si(111) atomic planes (separation 3.14 Å). The reciprocal lattice peaks, which were obtained from a 2D Fourier transform of the lattice-resolved image (inset in Figure 6a) and the diffraction pattern (inset in Figure 6b), proves that the growth axes is ⟨111⟩.

Cu as a catalyst leads to very effective growth of remarkably long Si-NWs. We never observed any catalytic particle atop, and the crystal quality is rather bad with a lot of stacking faults, but the growth direction is again unambiguously ⟨111⟩ (Figure 6c). For the tapered NWs catalyzed by Ag, typically axial twins parallel to the ⟨111⟩ growth axis along the entire length were observed (Figure 6d).

It is generally accepted that the conditions for VLS growth of NWs can be deduced from the binary phase diagrams involving the catalyst and Si. However, the growth temperatures with OCTS are lower than the lowest liquid eutectic of Pt/Si, Ni/Si, and Ag/Si shown on the bulk, and equilibrium phase diagram occurs at 979, 966, and 835 °C, respectively.

Even for Cu we achieved NW growth at 800 °C, which is the lowest temperatures for these catalyst where NWs could still be obtained, although raising the temperature improves their appearance. Furthermore, the size of our catalytic particles is still too big to produce a massive drop in the melting temperature.[33] We therefore suggest that the catalyst particle is in the solid state during our growth of Si-NWs, and that a solid-phase diffusion process either in the bulk, on the surface, or both, must be responsible for NW nucle-

DOI: 10.1021/nl101744q | *Nano Lett.* **2010,** *10,* 3957--3961

ation. Nominally subeutectic NW synthesis using Au as catalyst has been achieved for several semiconductor materials, including Ge,[34] InP,[35] GaAs,[36] and ZnSe.[37] For Si-NWs synthesis, our findings are conceptually similar to a previous report by Kamins et al.[38] of Ti-promoted Si-NW growth for temperatures below the Si−Ti eutectic point.

Concluding, for the new Si precursor OCTS we optimized synthesis parameters for Si-NW growth for Au, Pt, Ni, Ag, and Cu as catalyst. With increasing knowledge acquired during this work, epitaxial growth was achieved for Au, Ni, and Pt.

Acknowledgment. This work is partly funded by the Austrian Science Fund (Project No. 20937-N14) and the Austrian Society for Micro- and Nanoelectronics (GMe). We thank the Spawnt Research-Team, Bauch, C., Deltschew R., Holl, S., Lippold G., and Mohsseni, J. for development and supply of oligosilane precursors. TEM investigations by USTEM TU-Wien are gratefully acknowledged.

REFERENCES AND NOTES

(1) Cui, Y.; Wei, Q.; Park, H.; Lieber, C. M. *Science* **2001**, *293*, 1289.
(2) Duan, X. F.; Huang, Y.; Cui, Y.; Wang, J. F.; Lieber, C. M. *Nature* **2001**, *409*, 66.
(3) Orlov, A. O.; Amlani, I.; Bernstein, G. H.; Lent, C. S.; Snider, G. L. *Science* **1997**, *277*, 928.
(4) Baxter, J. B.; Aydil, E. S. *Appl. Phys. Lett.* **2005**, *86*, No. 053114.
(5) Valden, M.; Lai, X.; Goodman, D. W. *Science* **1998**, *281*, 1647.
(6) Brus, L. *J. Phys. Chem.* **1994**, *98*, 3575.
(7) Yorikawa, H.; Uchida, H.; Murmatsu, S. *J. Appl. Phys.* **1996**, *79*, 3619.
(8) Mozos, J. L.; Machado, E.; Hernandez, E.; Ordejon, P. *Int. J. Nanotechnol.* **2005**, *2*, 114.
(9) Pan, H.; Lim, S.; Poh, C.; Sun, H.; Wu, X.; Feng, Y.; Lin, J. *Nanotechnology* **2005**, *16*, 417–421.
(10) Wang, N.; Tang, Y. H.; Zhang, Y. F.; Lee, C. S.; Lee, S. T. *Phys. Rev.* **1998**, *B 58*, R16024.
(11) Harmand, J. C.; Tchernycheva, M.; Patriarche, G.; Travers, L.; Glas, F.; Cirlin, G. *J. Cryst. Growth* **2007**, *301−302*, 853–856.
(12) Westwater, J.; Gosain, D. P.; Tomiya, S.; Usui, S. *J. Vac. Sci. Technol., B* **1997**, *15*, 554–557.
(13) Wagner, R. S.; Ellis, W. C. *Appl. Phys. Lett.* **1964**, *4*, 89.
(14) Dan, A.; Chakravorty, D.; Banerjee, S. *J. Mater. Sci.* **2002**, *37*, 4261–4271.
(15) Cui, Yi.; Lauhon, L. J.; Gudiksen, M. S.; Wang, J.; Lieber, C. M. *Appl. Phys. Lett.* **2001**, *78*, 2214.
(16) Hochbaum, A. I.; Rong, F.; Rongrui, H.; Peidong, Y. *Nano Lett.* **2005**, *5*, 457–460.
(17) Park, W. I.; Zheng, G.; Jiang, X.; Tian, B.; Lieber, C. M. *Nano Lett.* **2008**, *8*, 3004–3009.
(18) Schmidt, V.; Senz, S.; Gösele, U. *Nano Lett.* **2005**, *5*, 931.
(19) Lugstein, A.; Hyun, Y. J.; Steinmair, M.; Dielacher, B.; Hauer, G.; Bertagnolli, E. *Nanotechnology* **2008**, *19*, 485606.
(20) Ge, S.; Jiang, K.; Lu, X.; Chen, Y.; Wang, R.; Fan, S. *Adv. Mater.* **2005**, *17* (1), 56–61.
(21) Sharma, S.; Kamins, T. T.; Williams, R. S. *J. Cryst. Growth* **2004**, *267*, 613.
(22) Islam, M. S.; Sharma, S.; Kamins, T. I.; Williams, R. S. *Nanotechnology* **2004**, *15*, L5–L8.
(23) Jagannathan, H.; Deal, M.; Nishi, Y.; Woodruff, J.; Chidsey, C.; McIntyre, P. C. *J. Appl. Phys.* **2006**, *100*, No. 024318.
(24) Lugstein, A.; Andrews, A. M.; Steinmair, M.; Hyun, Y. J.; Bertagnolli, E.; Weil, M.; Pongratz, P.; Schramböck, M.; Roch, T.; Strasser, G. *Nanotechnology* **2007**, *18*, 355306.
(25) Ge, S.; Jiang, K.; Lu, X.; Chen, Y.; Wang, R.; Fan, S. *Adv. Mater.* **2005**, *17* (1), 56.
(26) Walsh, R. *Acc. Chem. Res.* **1981,** *14,* 246−252.
(27) Ezhov, Y. S.; Simonenko, E. P.; Sevastyanov, V. G. *Russ. J. Phys. Chem.* **2009**, *A 83*, 179–181.
(28) Wang, N.; Zhang, Y.; Zhu, J. *J. Mater. Sci. Lett.* **2001**, *20*, 89–91.
(29) Habuka, H.; Suzuki, T.; Yamamoto, S.; Nakamura, A.; Takeuchi, T.; Aihara, M. *Thin Solid Films* **2005**, *489*, 104–110.
(30) Allen, J. E.; Hemesath, E. R.; Perea, D. E.; Lensch-Falk, J. L.; Li, Z. Y.; Yin, F.; Gass, M. H.; Wang, P.; Bleloch, A. L.; Palmer, R. E.; Lauhon, L. J. *Nat. Nanotechnol.* **2008**, *3* (3), 168–173.
(31) Wang, Y. W.; Schmidt, V.; Senz, S.; Gösele, U. *Nat. Nanotechnol.* **2006**, *1*, 186–189.
(32) Colombo, C.; Spirkoska, D.; Frimmer, M.; Abstreiter, G.; Fontcuberta i Morral, A. *Phys. Rev. B* **2008**, *77*, 155326.
(33) Buffat, P.; Morel, J. P. *Phys. Rev. A* **1976**, *13*, 2287.
(34) Greytak, A. B.; Lauhon, L. J.; Gudiksen, M. S.; Lieber, C. M. *Appl. Phys. Lett.* **2004**, *84*, 4176.
(35) Dick, K. A.; Deppert, K.; Martensson, T.; Mandl, B.; Samuelson, L.; Seifert, W. *Nano Lett.* **2005**, *5*, 761.
(36) Persson, A. I.; Larsson, M. W.; Stenström, S.; Ohlsson, B. J.; Samuelson, L.; Wallenberg, L. R. *Nat. Mater.* **2004**, *3*, 677.
(37) Colli, A.; Hofmann, S.; Ferrari, A. C.; Ducati, C.; Martelli, F.; Rubini, S.; Cabrini, S.; Franciosi, A.; Robertson, *J. Appl. Phys. Lett.* **2005**, *86*, 153–103.
(38) Kamins, T. I.; Williams, R. S.; Basile, D. P.; Hesjedal, T.; Harris, J. S. *J. Appl. Phys.* **2001**, *89*, 1008.

DOI: 10.1021/nl101744q | *Nano Lett.* **2010,** *10,* 3957--3961